Effects Of Inverter Clipping On Solar Power Variability

Mónica Zamora Zapata[1,2], Eduardo Luccini[3,4], Mauricio Trigo-González[2,5], Jorge Rabanal-Arabach[2,5]

[1] Departamento de Ingeniería Mecánica, Universidad de Chile, Santiago (Chile)

[2] Solar Energy Research Center, SERC, Santiago, (Chile)

[3] CONICET-CEPROCOR, Sede Santa María de Punilla, Córdoba, (Argentina)

[4] Facultad de Química e Ingeniería del Rosario, Pontificia Universidad Católica Argentina, Rosario (Argentina)

[5] Centro Desarrollo Energético Antofagasta, CDEA, Universidad de Antofagasta, Antofagasta (Chile)

Abstract

Inverter clipping applies to photovoltaic systems with a solar power capacity greater than the inverter output, mitigating the incoming solar variability while losing a surplus in solar energy production. We study the effects of inverter clipping on solar power generation variability by modeling a PV system with monofacial or bifacial modules, fixed tilt and tracking, using solar data for Boulder, CO, and assessing the resulting solar power generation with a novel dimensionless variability index (DVI). Comparing the output AC to the input DC power, annual averages of daily DVI diminish between 4% and 15%, the greater for bifacial modules. We analyze the direct effect of the inverter-to-load ratio (ILR) for two selected days with little and large variability. Generated power variability decreases after a given ILR value for each configuration, under a systematic behavior: at high ILR, variable days deliver more AC energy with lower variability for fixed tilted configurations. For clear sky days, this occurs for tracking configurations.

Keywords: PV Energy Generation, Solar Variability, Inverter-to-Load ratio, Inverter Clipping

1. Introduction

Solar irradiance intensity at the Earth's surface is variable across different timescales, with yearly and daily variations according to the seasons and motion of the Earth, and shorter scales related to meteorology, where passing clouds or aerosols impact the resulting surface solar irradiance. When converting solar irradiance into solar photovoltaic (PV) power, the configuration of the PV system, including its inverter, and environmental conditions, determine the generated power and its resulting variability.

One main variable in the configuration of a PV system is the inverter-to-load ratio (ILR) or DC/AC ratio, the proportion between the total PV DC power capacity and the inverter output AC power capacity. As PV panel costs have decreased in the last decade, newer solar farms have increased their ILR (EIA, 2018). A larger ILR can increase the solar AC power production during winter, and operate at the maximum AC output power during summer, an effect known as "inverter clipping", where the excess solar production is known as "clipping losses" (Kharait et al., 2020). These combined effects of increasing ILR result in a nonlinear relationship between ILR and the energy yield, for which an optimal ILR can be found (Deschamps and Rüther, 2019; Bahloul and Khadem, 2024). Bifacial PV systems, which currently dominate the utility-scale market (Stein et al., 2024), strongly influence clipping losses and greater energy production (de Souza Silva et al., 2021). Most existing studies focus on energy yield and clipping losses, and little attention is given to the resulting solar power variability, which the clipping effect could mitigate.

In this work, we study the effects of inverter clipping on solar power variability by simulating a PV system under various configurations. We consider monofacial and bifacial modules and vary the ILR with a fixed inverter model. We analyze the resulting solar power, calculate variability indicators, and their relationship to the PV configuration and ILR.

10.18086/swc.2025.04.17 Available at http://proceedings.ises.org

2. Data and methods

2.1. Photovoltaic system configuration and simulation

The simulation setup closely follows previous work (Zamora Zapata et al., 2023), where the PV system is modeled after Ladd (2018). It consists of 5 strings of 19 monofacial Yingli 330 W modules connected to a 30 kW SMA inverter, with a resulting ILR of 1.05. We consider a comparable bifacial system based on Ayala Pelaez et al. (2019), with five strings of 22 Silfab 285 W PV modules connected to the same 30 kW SMA inverter, matching the ILR of 1.05. For each system, we vary the ILR through the number of PV modules.

We use surface solar measurements for 2020 at Boulder, CO, from the SURFRAD network, which includes global horizontal, diffuse, and direct irradiance with a 1-minute frequency. This site is located at a high altitude and is well known for the presence of different cloud types, therefore useful for assessing variability.

The solar power simulation is performed with *pvlib* (Holmgren et al., 2018), where we calculate the plane-of-array irradiance from the direct and diffuse components using the Perez transposition model, and the PV module output using the single diode CEC model and the NOCT temperature. All losses are set to zero, as a worst-case scenario for output variability. The bifacial irradiance is calculated with *pvfactors*, using a row height of 2 m, a panel length of 1.5 m, and a ground-to-cover ratio of 0.35, following Ayala Pelaez et al. (2019).

We test a total of six different system configurations that result from combining orientation and module configuration. Two possible orientation systems are considered: a fixed tilt of 25º facing South, and a Horizontal Single Axis Tracking (HSAT) system. Three possible module configurations are considered: a monofacial module, a bifacial module with the site mean albedo (0.199), and a bifacial module with an enhanced albedo (0.6).

2.2. Measuring solar variability

A diverse set of solar variability metrics exists, based on either signal statistics, ramp rates, or geometric representations. An example of the latter is the variability index (*VI*), proposed by Stein et al. (2012), where the Euclidean length of the measured solar irradiance is compared to that of the clear sky irradiance. Similarly, Kreuwel et al. (2020) proposed a power variability index for PV systems, which can be calculated using either the power before the inverter (DC power) or after the inverter (AC power) for a whole day, and is normalized by the daily energy production, as

$$VI = \frac{\sum_{k=2}^{n} \sqrt{\left(P_k - P_{k-1}\right)^2 + \Delta t^2}}{E_{day}}, \qquad \text{(eq. 1)}$$

where P is the solar power (kW), before or after the inverter, $\Delta t = t_{k-1} - t_k$ is the time series resolution or interval between measurements (h), n is the number of time intervals within a day, and E_{day} is the daily solar energy (kWh), also named surface integral in Kreuwel et al. (2020).

Both variability index metrics, proposed by Stein et al. (2012) and Kreuwel et al. (2020), have a potential consistency flaw, since they aren't nondimensional. In fact, as given in eq. (1), *VI* has units of $\frac{\sqrt{kW^2+h^2}}{kWh}$. This means that measurements with different time resolutions will result in different ranges of variability indices, and therefore, caution must be taken when used for comparison purposes. This is particularly concerning for the units used: if *VI* is calculated with Δt in (h) or (min), or if power is considered in (W) or (kW), it will deliver different values. Kreuwel et al. (2020) tried to address this issue by normalizing the obtained *VI* values with the maximum in the dataset, effectively resulting in a metric between 0 and 1. We propose an alternate method to calculate a true nondimensional metric inspired by the variability index, which we call the dimensionless variability index (*DVI*), where instead of adding the squared difference of power to the squared difference of time, which was the geometric inspiration for Stein et al. (2012), we multiply these terms to match the energy units.

$$DVI = \frac{\sum_{k=2}^{n} \Delta t \left|P_k - P_{k-1}\right|}{E_{day}} \qquad \text{(eq. 2)}$$

The DVI is consistent using different time or power units. From eq. (2), we can also interpret the DVI as the sum of the absolute power difference normalized by a reference power, which would be $P_{ref} = \frac{E_{day}}{(n-1)\,\Delta t}$, since Δt is usually constant.

2.3. Clipping events

We assess the occurrence of clipping events by filtering the lapse where the AC power is constant and equal to the nameplate power capacity of the inverter. Following this criterion, we assess both the daily total clipping time, t_{clip}, and the daily number of clipping events, n_{clip}.

3. Results and discussion

3.1. Sample effects of inverter clipping

The effect of inverter clipping is notorious when observing the time series of DC and AC power in Fig. 1. For the tilted configuration, clipping is present around noon, and for the HSAT, it extends for a longer period. The bifacial case with a high albedo is also subjected to more clipping, due to a sustained higher power.

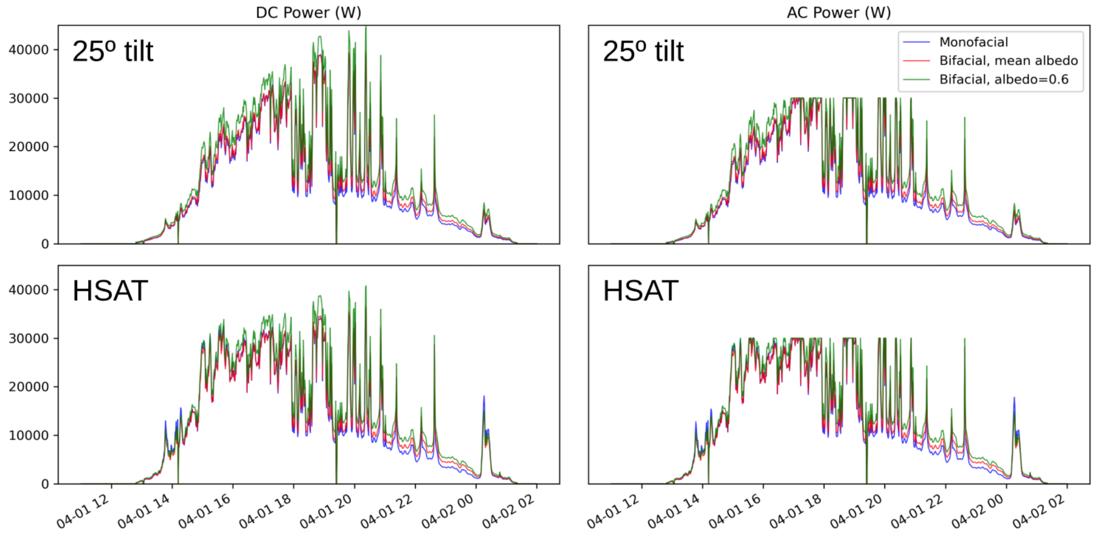

Fig. 1: Analysis for April 1st. The left column shows the DC power, and the right column shows the AC output with inverter clipping, in W. The top row is for 25° tilt cases, and the bottom row is for HSAT cases.

3.2. Annual analysis of daily variability

When looking at the whole year, Fig. 2 shows that the days have a wide distribution in the VI or DVI versus energy space, representing the diverse cloudy conditions in Boulder, and resembling the variety of conditions analyzed by Kreuwel et al. (2020). Monofacial systems with an HSAT configuration can generally lead to higher variability. In this case, both VI and DVI were calculated with the following units: time in (h) and power in (kW). Although the values of VI and DVI differ due to their definition, the space distribution seems nearly identical.

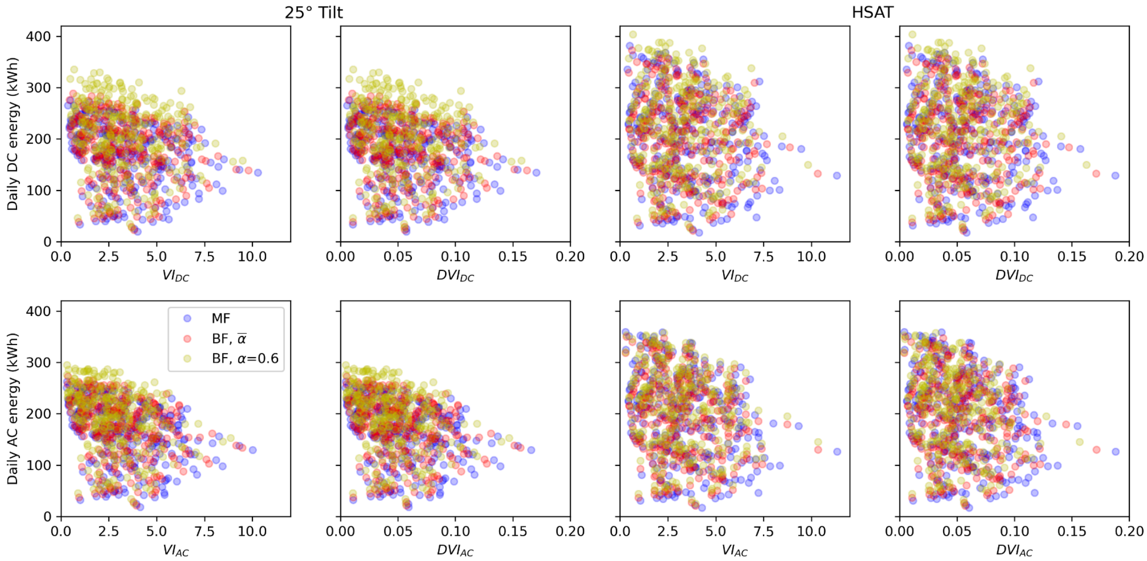

Fig. 2: Daily *VI* and *DVI* for all simulated configurations. The top row shows the DC power, and the bottom row shows the AC output with inverter clipping. The left columns correspond to a 25° tilt, and the right columns to an HSAT configuration.

We further assess the similarity between *VI* and *DVI* in Fig. 3, which shows a striking linear relationship between both metrics, further validating the use of *DVI* as a proper dimensionless parameter. If *VI* and *DVI* were calculated using different units, such as time in (min) and power in (W), we find that the linear fit would be even better (not shown), since the absolute values of power are around two orders of magnitude greater than those of time, therefore, weighting little in the square root term for *VI*.

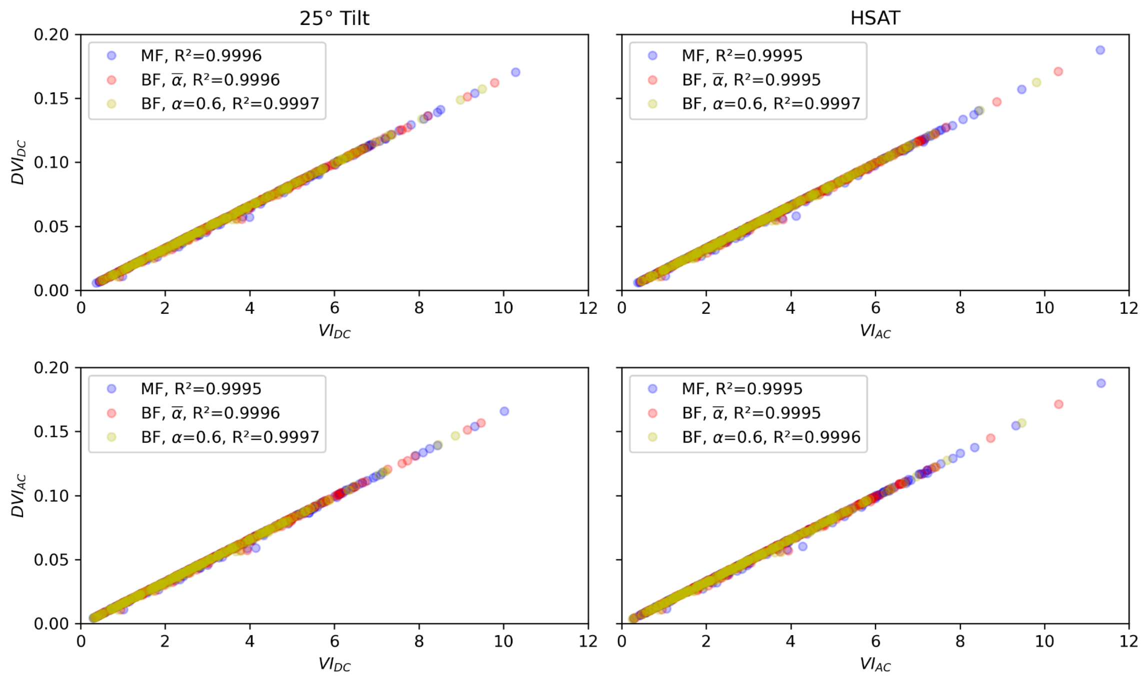

Fig. 3: Comparison between daily VI and DVI for DC and AC power, and for the 25º tilt and HSAT configurations.

Table 1 shows the statistics of both *VI* and *DVI*, showing that both the DC and AC solar power variability can be reduced for bifacial systems when compared to the monofacial case. Therefore, bifacial systems that display inverter clipping can mitigate some solar power variability, and the net effect depends on both the tilt/tracking configuration and ground albedo. When assessing the effect of inverter clipping alone on variability, by contrasting DC and AC metrics, we see a reduction that is greater for the bifacial case, with nearly 12% less variability for the HSAT configurations and 15% for the fixed tilt cases. Overall, for this site, the lowest mean variability is achieved for bifacial modules with enhanced albedo in a fixed tilt configuration.

Table 1 - Mean VI and DVI statistics for all days in 2020.

	25º Tilt			HSAT		
Mean VI $\left(\frac{\sqrt{kW^2+h^2}}{kWh}\right)$	**DC**	**AC**	**Diff.**	**DC**	**AC**	**Diff.**
Monofacial	3.36	3.18	-5.3%	3.56	3.42	-3.9%
Bifacial, mean α	3.31	3.10	-6.3%	3.40	3.25	-4.3%
Bifacial, α=0.6	3.28	2.78	-15.2%	3.30	2.91	-11.8%
Mean DVI (-)	**DC**	**AC**	**Diff.**	**DC**	**AC**	**Diff.**
Monofacial	0.055	0.052	-5.5%	0.058	0.056	-4.1%
Bifacial, mean α	0.054	0.051	-6.6%	0.056	0.053	-4.5%
Bifacial, α=0.6	0.054	0.045	-15.8%	0.054	0.048	-12.2%

3.4. Analysis of clipping events

While modern control systems for inverters and PV arrays should be able to handle clipping events, it is still of interest to observe how frequent and lasting they can be for each day, in all the considered configurations. Figures 4 and 5 present the number of clipping events, n_{clip}, and the total daily clipping time, t_{clip}, for the whole year, with respect to both daily AC energy and DVI_{AC}. Even though the ILR of the basic configuration studied here is relatively low (1.05), there are days with over 9 h of clipping.

The number of clipping events is greater for the HSAT configurations, and it also grows when having bifacial modules with enhanced albedo. In other words, the number of clipping events depends more on the daily energy than on variability, which is expected, as lower energy days, likely to have a lower maximum power, are not as susceptible to clipping.

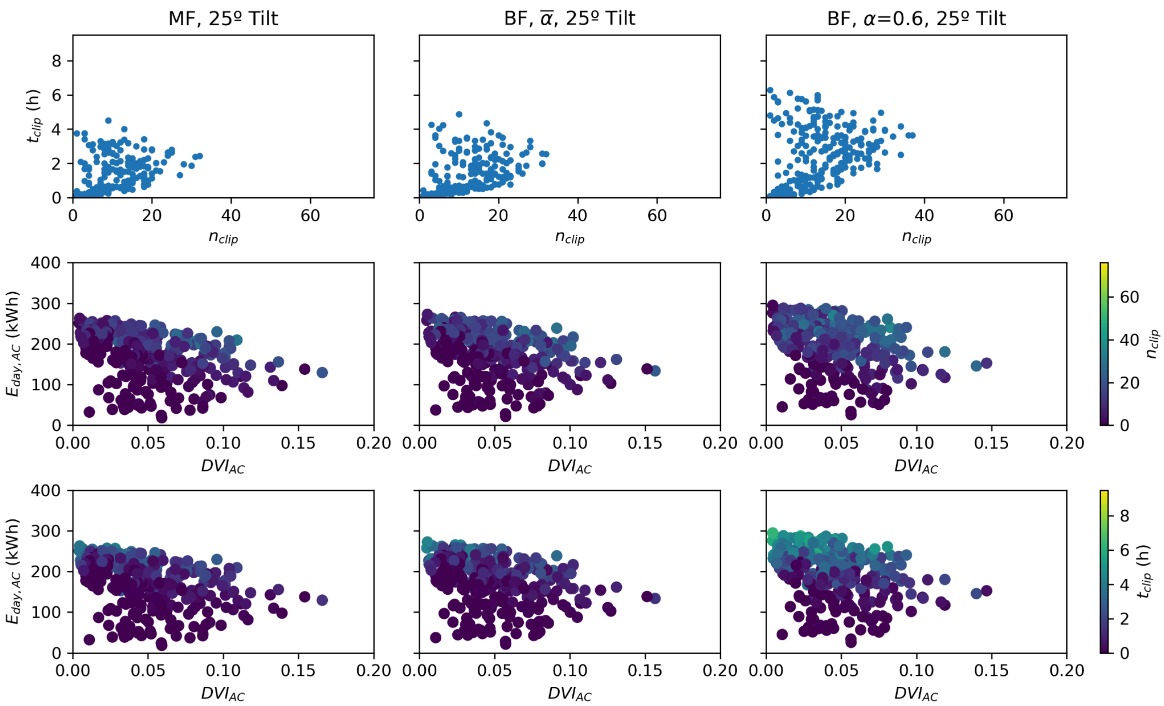

Fig. 4: Analysis of the number of clipping events and total clipping time for the 25º tilt cases.

A similar behavior is observed for the total clipping time; it is longer for days with a greater daily energy, with the largest values occurring for HSAT configurations, as we expect longer periods of the day may reach a higher plane-of-array irradiance. Though both clipping metrics have a relationship with the daily energy, only for the HSAT cases do we see a glimpse of a linear relationship with each other, with considerable dispersion.

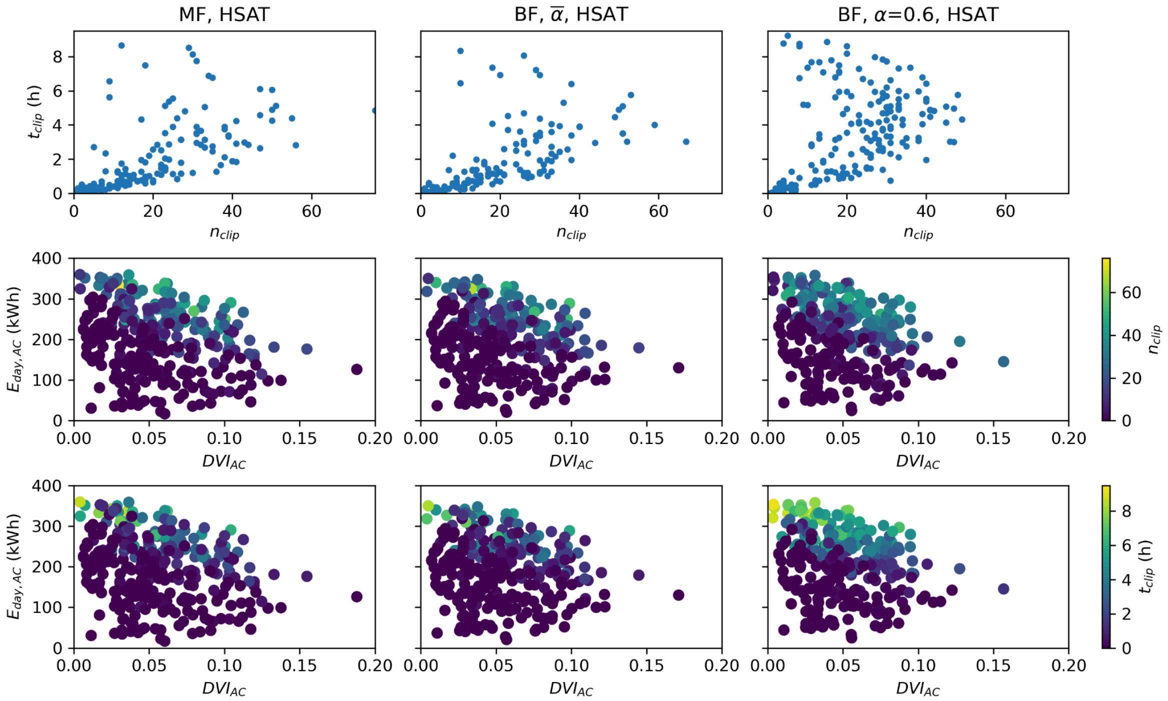

Fig. 5: Analysis of the number of clipping events and total clipping time for the HSAT cases

3.5. Effects of changing the ILR for selected days

We now analyze the effects of modifying the ILR on power variability. In order to assess this relationship, we look at two particular days in the MF 25° tilt configuration, since it has greater variability: the one with the largest DVI_{DC}, September 20th, and the one with the lowest DVI_{DC}, April 7th. Their respective solar GHI irradiance is shown in Fig. 6, where it is evident that September 20th has intense cloud-induced variability throughout the whole day, while April 7th corresponds to a clear sky day.

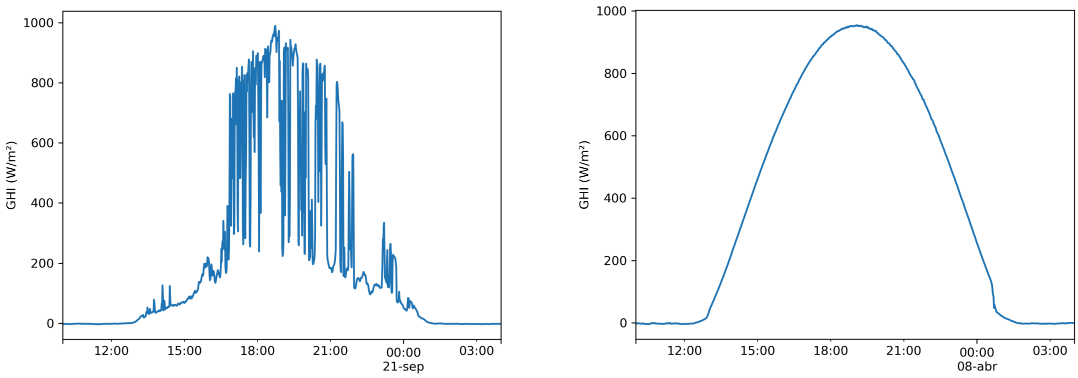

Fig. 6: Solar global horizontal irradiance for September 20th (left) and April 7th (right).

We modify the ILR in each system by changing the number of PV modules per string; in the case of monofacial modules, this range was 15 to 25 modules, while for the bifacial case, it was 18 to 28 modules. Fig. 7 shows the resulting variability and daily energy for different ILR values in the high variability case of September 20th. The daily energy always grows with ILR, as adding more modules increases the available power throughout the day. This energy increase is linear for DC power, and nonlinear for AC power: the increased slope then slows with higher ILR, an expected effect of inverter clipping. While DVI_{DC} is not affected by the change in ILR, DVI_{AC} is constant until it reaches a critical value, after which it decreases linearly with ILR. Even though the critical ILR differs for each configuration, the linear decreasing slope is similar for all cases.

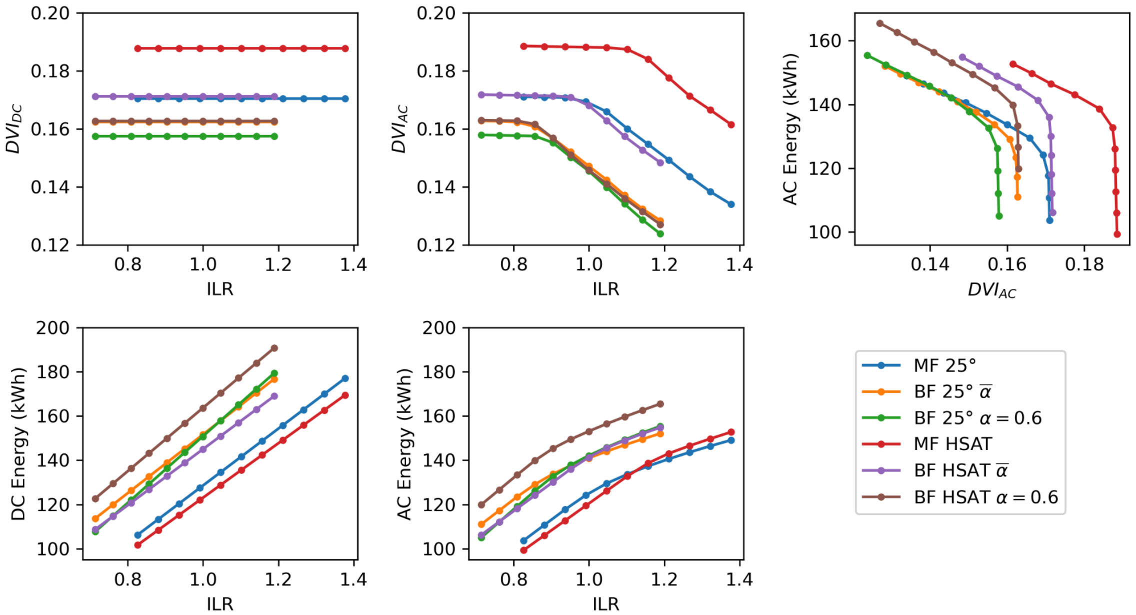

Fig. 7: Dependence of DVI and daily energy on ILR for September 20th.

Fig. 8 shows the influence of ILR on the low variability case, April 7th. The daily energy also grows in this case, but the increase is much reduced for AC power, since a clear day will reach a point where increasing PV modules will slowly add a few minutes of flat AC generation due to inverter clipping. While DVI_{DC} is slightly affected by the change in ILR, with very low variability, DVI_{AC} is constant until it reaches a critical value, after which it strongly decreases to an even lower range of variability with ILR. In this case, the critical ILR also differs for each configuration, but the decreasing slope is a bit different than that of September 20th; fixed tilt cases follow an exponentially decreasing trend, while the HSAT cases reach a constant DVI_{AC} after a strong change. This may not be as important in this case since all DVI values are quite small (0.003-0.008).

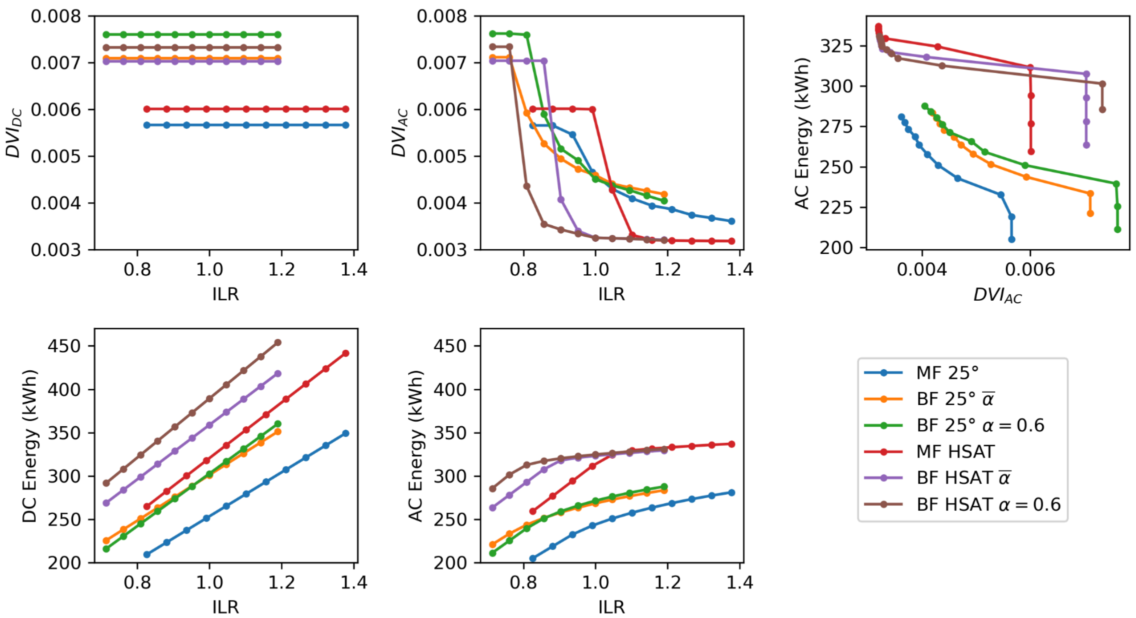

Fig. 8: Dependence of DVI and daily energy on ILR for April 7th.

For September 20th, the high variability day, the relationship between AC energy and DVI_{AC} (upper right panel in Fig. 7) is quite different from that of April 7th, the clear sky day (upper right panel in Fig. 8), as the family of curves corresponding to a fixed tilt is quite separate from those of HSAT. Note that for September 20th, if a greater energy yield with lowest variability is desired, any fixed tilt configuration with a high ILR would be recommended. However, for April 7th, the largest AC energy is obtained with HSAT configurations, and all cases with a high ILR collapse in a low DVI_{AC}. Therefore, an HSAT configuration would be recommended. This type of result could be a useful input for design purposes in locations with a known dominance of either variable or clear sky days. To determine how much a low variability configuration is valued, a techno-economic assessment could be performed by considering the sizing of a storage system to further mitigate solar generation variability.

4. Conclusions

We have studied the effects of inverter clipping on solar power generation variability by modeling the input and output power of an inverter under several PV system configurations for a full year in Boulder, CO. The PV system configuration consisted of monofacial and bifacial modules (a case with the site mean albedo, and a case with enhanced albedo), in either fixed tilt at 25º, or horizontal single-axis tracking systems.

We assessed the daily variability for each basic configuration, with an ILR of 1.05, by calculating the power variability index (Kreuwel et al., 2020), as well as a novel proposed dimensionless variability index (*DVI*). We find that bifacial systems display smaller variability indicators, due to enhanced inverter clipping that is visible by both a greater number of daily clipping events and total daily clipping time. We also show that the novel *DVI* metric is similar to the original variability index, validating its use under a conceptually robust dimensionless frame more easily interpretable with less dependence on the time interval considered. The resulting mean daily *DVI* is effectively lower when calculated with the output AC power compared to the input DC power, a reduction that ranges between 4-15% and peaks for bifacial systems.

We also studied the most and least variable days within the dataset by varying the number of PV modules to modify the ILR. For both days, we noted an increase in AC power production and that there is an ILR threshold, different for each configuration, after which the *DVI* begins to decrease. The way the decrease occurs is different for variable and smooth days, and interestingly, the relationship between daily total energy and variability also differs. While for the most variable day we can obtain more energy with little variability for fixed tilt configurations, for the least variable day, this happens for the tracking configuration. These results could be useful for designing PV systems at locations with either little variability or where strong variability dominates. Future research should expand on the variations of ILR for a larger set of days and locations, as well as to develop a techno-economic assessment on the benefits of reducing solar PV output variability.

5. Acknowledgements

This work was supported by SERC Chile (ANID grant FONDAP 1523A0006).

6. References

S. Ayala Pelaez, C. Deline, P. Greenberg, J. Stein, 2019. Model and Validation of Single-Axis Tracking With Bifacial PV. IEEE J. of Photovoltaics 9(3), pp. 715-721.

M. Bahloul, S. Khadem, 2024. A refined method for optimising inverter loading ratio in utility-scale photovoltaic power plant. Energy Reports, 12, 5110–5115.

J. de Souza Silva, K. de Melo, T. Costa, G. Vieira Machado, H. Moreira, M. Villalva, 2021. Impact of Bifacial Modules on the Inverter Clipping in Distributed Generation Photovoltaic Systems in Brazil. 2021 Brazilian Power Electronics Conference (COBEP), 1–6.

E. Deschamps, R. Rüther, 2019. Optimization of inverter loading ratio for grid connected photovoltaic systems. Solar Energy, 179, 106–118.

EIA. 2018. Solar plants typically install more panel capacity relative to their inverter capacity - U.S. Energy Information Administration (EIA). (accessed on 14 April 2025)

F. Holmgren, C. Hansen, M. Mikofski, 2018. pvlib python: a python package for modeling solar energy systems. Journal of Open Source Software, 3(29), 884.

R. Kharait, S. Raju, A. Parikh, M. A. Mikofski, and J. Newmiller, 2020. Energy yield and clipping loss corrections for hourly inputs in climates with solar variability. 47th IEEE Photovoltaic Specialists Conference (PVSC), pp. 1330–1334.

F. Kreuwel, W. Knap, W. van, J. Vilà-Guerau de Arellano, C. van Heerwaarden, 2020. Analysis of high frequency photovoltaic solar energy fluctuations. Solar Energy 206, pp. 381-389.

C. Ladd, 2018. Simulating NEC voltage and current values. SolarPro Magazine 11(4), pp. 12-18.

J. Stein, C. Hansen, M. Reno, 2012. The Variability Index; a new and novel metric for quantifying irradiance and PV output variability. SAND2012-2088C report.

J. Stein, G. Maugeri, N. Riedel-Lyngskær, S. Ovaitt, T. Müller, S. Wang, H. Huerta, J. Leloux, J. Vedde, M. Berwind, M. Bruno, D. Riley, R. Santhosh, S. Ranta, M. Green, K. Anderson, L. Deville, 2024. Best Practices for the Optimization of Bifacial Photovoltaic Tracking Systems. IEA Photovoltaic Power Systems Programme (PVPS).

M. Zamora Zapata, K. Lappalainen, A. Kankiewicz, J. Kleissl, 2023. Comparing solar inverter design rules to subhourly solar resource simulations. Journal of Renewable and Sustainable Energy, 15 (5), 053501.